Microporous Network-Assisted Formation of Copper-In-Polymer Gradient Composite Film

Bo Yang,[1] Jianguo Tang,[1] Peihua Yang,[1] Yao Wang,[1] Jixian Liu,[1] Haiyan Liu,[2]
Rui Wang,[1] Zhen Huang,[1] Jingquan Liu,[1] Laurence A. Belfiore[3]

[1]College of Chemistry, Chemical and Environmental Engineering, Institute of Hybrid Materials—the Growing Base
for State Key Laboratory, Qingdao University, Qingdao 266071, People's Republic of China
[2]College of Chemistry, Polytech University of East China, Shanghai 200000, People's Republic of China
[3]Department of Chemical and Bio Engineering, Colorado State University, Fort Collins, Colorado 80523

ABSTRACT: In this article, a copper-in-polymer-gradient composite film (CPGCF) was synthesized by electrochemical strategy via reducing a solvent-swollen cathode film (SCF). The latex nanoparticles of a ternary copolymer including styrene, butyl acrylate, and acrylic acid structural units play the key role to form well-graded copper distribution in this ternary copolymer matrix through the porous morphological structure developed by latex nanoparticle semimelt joining. The morphological structure along cross-section of CPGCF includes three layers: (1) a dense copper layer in ternary copolymer matrix whose most outside was originally attached to cathode in electrochemical reac-

tor, (2) a shrublike layer that grew from dense copper layer, and (3) a clear layer in which there is no obvious reduced copper phase whose most outside was originally contacted with liquid electrolyte medium in electrochemical reactor. As experimental aspects, the influences of emulsion polymerization conditions of ternary copolymer, predrying time and temperature of SCF, dc voltage in electrochemical reduction on CPGCF structure were investigated. © 2012 Wiley Periodicals, Inc. J Appl Polym Sci 000: 000–000, 2012

Key words: nanolatex film; copper; gradient; electrochemical reaction; composite

INTRODUCTION

The gradient composite materials, as described,[1] show their unique characteristics in properties via gradient concentration distribution of a component in matrix materials. Previously, metal-in-ceramic or metal-in-metal gradient materials were reported[2–5] for avoiding from thermal or bending stress breakage in layer structural composites deriving from single component materials. In this case, the composite is also free of cracks. Therefore, this structure can be available for any needs where the breakages will happen at their interface between two materials that

have different thermal shrinkage, elongation, mechanical strength, and so on.[6,7]

Following the inorganic gradient materials studies, the polymer matrix gradient composites emerged just in recent years because of the difficulty to treat the differences of processing conditions between polymers (normally at low temperature, lower than 300°C) and inorganic materials or metals (normally at high temperature, higher than 1000°C). Thus, the novel preparation methods have been exploited lately. For example, to enhance the wear resistance property of epoxy resin, carbon fiber-reinforced epoxy gradient composites were developed at different centrifugation speeds having 3 wt % of milled carbon fiber. Sample prepared at 900 rpm after the transition zone shows maximum wear resistance due to the presence of more number of carbon fibers.[8] Additionally, using a solution-cast route, the electroactive polymer membrane and platinum electrodes were fabricated onto the membrane through electroless plating. A finely dispersed platinum particle deeper and gradient penetrating within the near-boundary region with a smaller average particle size and more uniform distribution could be obtained through a reverse electroless plating.[9]

Our group has developed an electrochemical method, solution-reduction synthesis (SRS), by which a solvent-swollen cathode film (SCF) was

reduced into a copper-in polymer gradient composite film (CPGCF).[10,11] This method was easy to modulate the content, morphology, and distribution of metal-in-polymer. However, there are almost no existed polymers that can act as ideal polymer matrix in this special electrochemical system, because the transportation and reduction of copper ions (Cu^{2+}) in SCF are affected by complicated factors, such as ion saturation, electric potential for ion motion, and related electrochemical conditions.

In the recent years, the synthesized latex nanoparticles of copolymers have been found as structural templates. Velev[12] first made three-dimensional ordered antiopaline silicon dioxide materials using polystyrene latex film as templates based on the densely packed array forming in the second stage by keeping proper film-forming conditions (temperature, humidity, and so on).[13–15] Herein, we synthesized a ternary copolymer including styrene, butyl acrylate, and acrylic acid structural units, with which the porous structure agglomerated by its latex nanoparticles was developed. With the assistance of this porous structure, a CPGCF was prepared by electrochemical strategy via reducing a SCF made by this ternary copolymer latex.

EXPERIMENTAL

Materials

Styrene (St, C.R.), butyl acrylate (BA, C.R.), and acrylic acid (AA, C.R.) were purified by distillation under vacuum and stored in a refrigerator. Sodium dodecyl sulfate (SDS, C.R.), ammonium per sulfate (APS), and all of other inorganic chemicals were analytical grade reagents and used as received without further purification. Reagent copper sulfate ($CuSO_4$) was as ion resource in the electrolyte of sulfuric acid (H_2SO_4) in electrochemical reactor and was used as received.

Synthesis of poly(St-*co*-BA-*co*-AA) ternary copolymeric nanolatex

Poly(St-*co*-BA-*co*-AA) latex was prepared by a standard semibatch emulsion polymerization process using SDS as emulsifier, APS as initiator, and sodium bicarbonate ($NaHCO_3$) as buffer. Ternary poly(St-*co*-BA-*co*-AA) nanolatex was prepared by a standard semibatch emulsion polymerization process. Synthesis of poly(St-*co*-BA-*co*-AA) nanolatex was shown in Figure 1. First, water (75 g), SDS (1 g), $NaHCO_3$ (0.45 g), and 50% of the mixture [styrene (24 g), butyl acrylate (24 g), and acrylic acid (2 g)] were charged into a flask, which was then dipped in a 78°C water bath. After stirring at around 250 rpm for 0.5 h, 1/2 of APS (0.2 g) was introduced and polymerization reacted for 0.5 h. Then, the polymer-

ization was conducted by drop-wise addition of the left monomer mixture and the remnant APS in to the system, and the feed time was 4 h followed by an additional 3 h of aging. The final solid content in this polymerization was 40 wt %.

Preparation of SCF

Poly(St-*co*-BA-*co*-AA) latex was coated on a graphite electrode and dried at 25°C for about 30 h to get semiswelling coagulated nanolatex film. The volume of latex in coated electrode film was kept in the range of 6–16 mL to control thickness of the film.

Electrochemical reduction of SCF

The coagulated nanolatex film was reduced by SRS, which was established in our previous experiments.[1] The electrolytic system was composed of a copper anode, a graphite cathode that was coated with SCF, and liquid medium between the couple electrodes. The liquid medium was a mixed solution of copper sulfate, sulfuric acid, and water. The concentration of $CuSO_4$ was 150 g/L, and the quality ratio of $CuSO_4$ to H_2SO_4 in the electrolyte was 3 : 1. The electrochemical reactions were started at room temperature and kept for 9 h. The applied power voltage between two electrodes was constant and kept at 0.55 ± 0.5 V. After electrochemical reduction, the semiswelling coagulated nanolatex films were peeled off from cathode, washed by deionized water for five times, and dried at 70°C for 5 h.

Characterization

The morphology and size of poly(St-*co*-BA-*co*-AA) latex were measured on an H-600 transmission electron microscopy (TEM; Hitachi, Japan). The samples of diluted latex were dropped onto a copper grid. For better contrast of particle edges, a drop of phosphor-tungstic acid was placed on the grid.

Differential scanning calorimetry (DSC) study was conducted on a Mettler Tole Do 822 instrument working with 665 mg samples in aluminum pans. Runnings at constant heating rate of 10°C/min were performed in a temperature range 30–100°C.

The morphology in cross-section of semiswelling coagulate nanolatex film and CPGCF was tested by a scanning electronic microscope (SEM): A Cambridge Instrument S250MK IV (Japan). The samples used in tests were broken into thin and long pieces, adhered to a sample frame, and spattered with gold.

The morphology in the cross-section of CPGCF was also tested by a Nikon E 600 (POL/EMS-600, Japan) polarized optical microscope (POM). The sample used in the test was dried completely and broken into thin and long pieces, adhered to the sample frame.
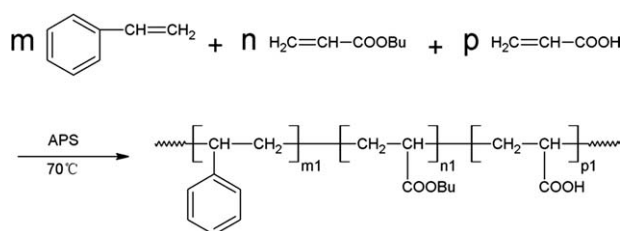
Figure 1 Illustration of synthesis reaction of poly (St-*co*-BA-*co*-AA) nanolatex.

X-ray diffraction (XRD, Bruke D8, Germany) was used for copper (0) measurement. The copper content evaluation was finished by energy-dispersive spectrometry (EDS) under SEM (Cambridge Instrument S250MK IV, Japan), through capturing the sample cathode side in 2.5 × 3.5 mm, and the element contents were collected from this EDS spectrum. XPS measurement was on a VG Scientific ESCALab220i-XL, for which Mg Kα X-ray was as excited resource (300 W), and vacuum was at 3×10^{-9} mbar.

RESULTS AND DISCUSSION

Micromorphological structure of coagulated nanolatex film

Styrene, butyl acrylate, and acrylic acid act as different role for this copolymer. Styrene contributes its
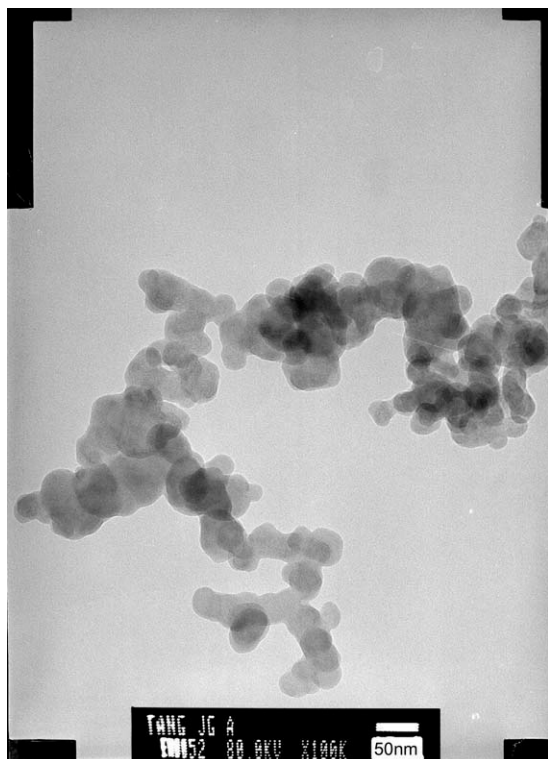
hard property with amorphous structure in polymer, butyl acrylate contributes its low glass transition temperature, and acrylic acid imparts the electrolyte character to the copolymer. Therefore, the copolymer constructed by these three monomers is expected to have enough shape maintainability, softness at room temperature, and hydrophilicity. This ternary copolymer was synthesized by semibatch emulsion polymerization strategy that was described in Experimental section. The obtained product is fine latex with the well-emulsified polymer particles in nanoscale diameter. A TEM micrograph of this latex was shown in Figure 2, in which spherelike particles with about 50 nm diameter conglomerate into irregular architecture after aqueous medium evaporates.

Figure 3 shows the morphological structure of a semidrying casting latex film that coagulated in room temperature. The porous structure with submicron backbone network is clear. The pores have 1–5 μm diameter, and the backbone width is about 100–500 nm. It is believable that this conglomeration of latex nanoparticles should follow the literature-suggested mechanism[16–19]: (1) evaporation of medium from latex bulk, (2) shrinkage of distances among latex particles, and (3) evaporation of interstice medium among densely packed immobile spheres. Naturally, the apparent volume shrinkage makes the casting latex form the coagulated structure. However, the porous structure is unbelievable following the above coagulation mechanism. Obviously, the backbone network develops with the nonunique shrinkage occurrence inside the casting latex. As shown in Figure 2, the ternary latex nanoparticles tend to conglomerate into irregular architecture, in which the
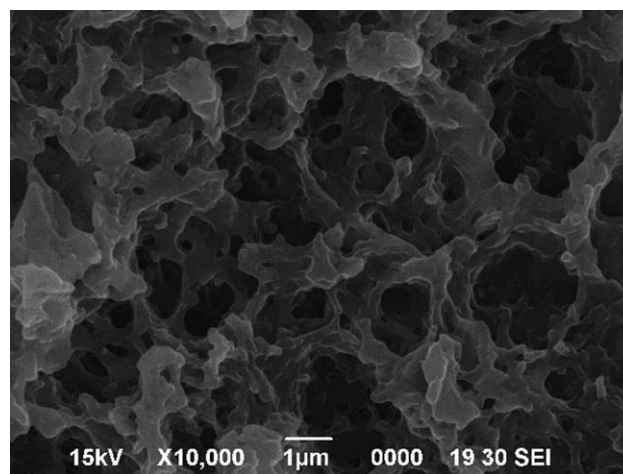

Figure 2 Transmission electron microscope (TEM) micrograph of P(St-*co*-BA-*co*-AA) nanospheres. The latex was diluted to solution of 0.5 wt % before measurement.

Figure 3 Morphological structure in the section of semi-swelling coagulated nanolatex film obtained by SEM. Fourteen milliliters of latex were coated on a graphite electrode and was dried at 25°C for about 30 h to get semi-swelling coagulated nanolatex films. After peeling the films from the electrode, they were cooled at −25°C for 1 h and broke into thin and long pieces before testing.
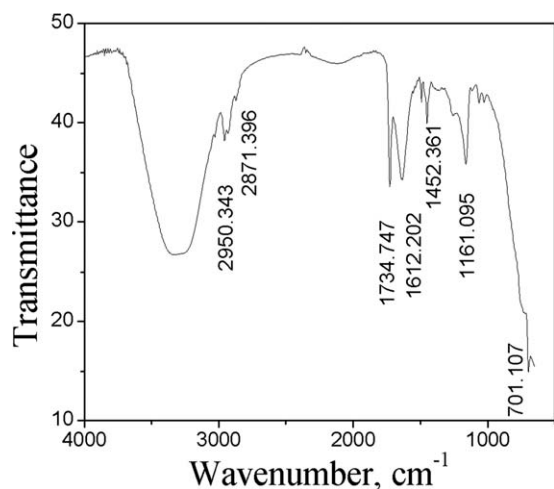
Figure 4 FTIR spectrum of poly(St-*co*-BA-*co*-AA) film.

width of backbone is similar to that in this backbone network in Figure 3. However, one can find that the backbone in the network structure is a solid architecture that fully loses the spherical shape originating from its parent latex nanoparticles. This means the felting among parent latex nanoparticles. Figure 4 shows FTIR spectrum of poly(St-*co*-BA-*co*-AA) film. The peaks at 2950, 2871, 1734, and 1452 cm^{-1} are associated with the characteristic vibration of methyl (—CH$_3$), methylene (—CH$_2$), carbonyl (C=O), and methyl (—CH$_3$). The peaks at 1612 and 701 cm^{-1} are characteristic absorption peaks of benzyl groups. The peaks at 1161 cm^{-1} are characteristic absorption peaks of C—O—C bonds. These results prove that the copolymerization among three monomers has been

taken place adequately. Figure 5 shows the DSC curve of this ternary copolymer, which indicates that the T_g of the ternary copolymer is 11°C. This means that the copolymer situated at a semimelting status when it was dried at 25°C. Therefore, the pores were formed in the process of latex nanoparticle jointing each other. Pekcan ever reported poly(methylmethacrylate) (PMMA) latex,[20] but there is no porous structure being found. Obviously, PMMA does not have the low T_g character.

Micromorphological structure and composition of CPGCF

The cross-section of CPGCF was observed by both SEM (Fig. 6) and POM (Fig. 7). The photographs both show the gradient distribution of reduced copper along the observed cross-section from cathode side to the other. This gradient morphological structure of CPGCF can be described as (1) a dense copper layer (layer 1 in Figs. 6 and 7) in ternary copolymer matrix whose most outside was originally attached to cathode in electrochemical reactor, (2) a shrublike layer (layer 2 in Figs. 6 and 7) that grew from dense copper layer, which should result from the effect of point discharge, and (3) a clear layer (layer 3 in Figs. 6 and 7) in which there is no obvious reduced copper phase whose most outside was originally contacted with liquid electrolyte medium in electrochemical reactor. In both Figs. 6 and 7, there were no porous structure being found, because the sample experienced the drying treatment at 70°C for 5 h, in which all pores closed. The gradient distribution of reduced copper in
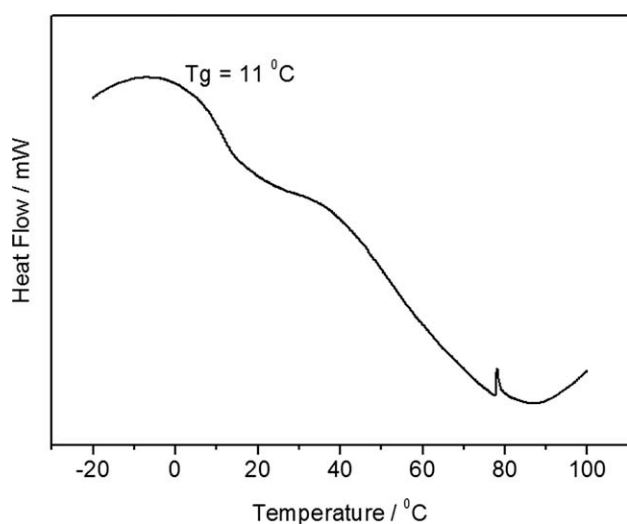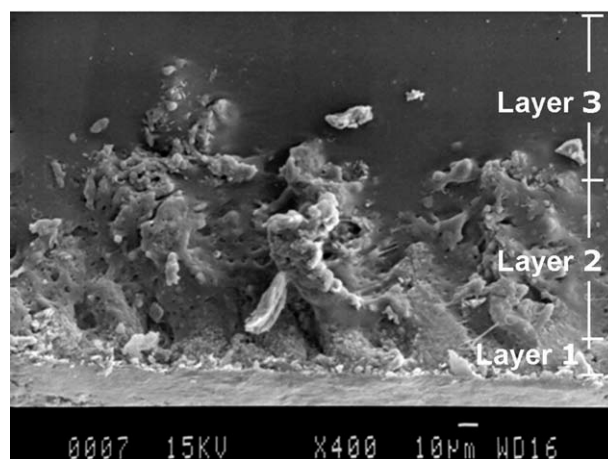

Figure 5 DSC of semiswelling coagulated nanolatex films. First, 14-mL latex was coated on a piece of glass and dried at 25°C to get dry latex films, then they were cut into grains, and 665 mg samples were put into aluminum pans for measurement. Runnings at constant heating rate of 10°C/min were performed in a temperature range −30 – 100°C.

Figure 6 Morphological structure of CPGCF obtained by SEM. Fourteen milliliters of latex were coated on a graphite electrode and dried at 25°C for about 30 h to get semiswelling coagulated nanolatex films. The voltage of direct electric power, 0.6 V; the electrochemical reduction time, 10 h; ratio of CuSO$_4$ to H$_2$SO$_4$ in the electrolyte, 3 : 1; the temperature in electrochemical reactor, 20°C; the electrode material, graphite.
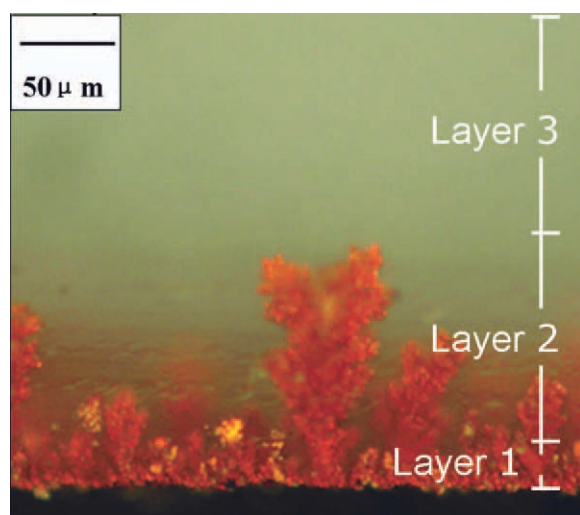
Figure 7 Morphological structure of CPGCF obtained by polarized optical microscope (POM). Sample was synthesized at the same conditions as in Figure 6. [Color figure can be viewed in the online issue, which is available at wileyonlinelibrary.com.]

cross-section of CPGCF is determined by Cu^{2+} motion in coagulated latex film that is a semi-SCF, in which there were no Cu^{2+} ions inside SCF originally. To get the reduced copper in the copolymer matrix, Cu^{2+} ions have to move through the SCF toward cathode and are reduced probably on the way to move. This transportation character of Cu^{2+} ions makes the dependence on the morphological structure of SCF. Referred to Figure 3, the porous structure in SCF is advantage for Cu^{2+} to migrate in SCF. The large porous volume fraction makes the short thickness of Cu^{2+} ions to penetrate within
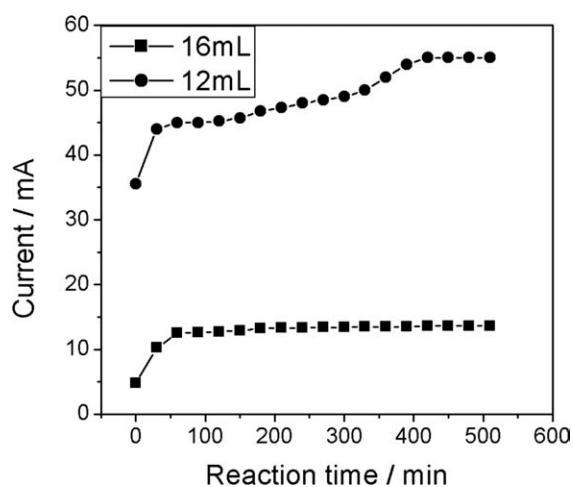

Figure 8 The influence of latex film thickness on reduction current. Synthesized conditions: predrying time of the coagulated nanolatex film, 30 h; the voltage of direct electric power, 0.60 V; concentration of $CuSO_4$, 150 g/L; ratio of $CuSO_4$ to H_2SO_4 in the electrolyte, 3 : 1. The thicknesses were indicated by the solution volumes (16 and 12 mL) used in casting SCFs.
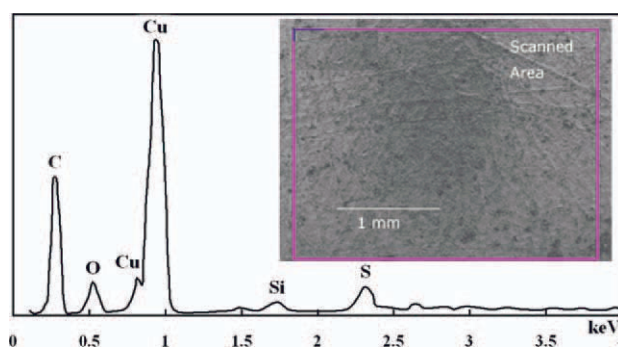

Figure 9 Energy-dispersive spectrometer (EDS) graph of CPGCF under SEM measurement. Sample was synthesized at the same conditions as in Figure 6. [Color figure can be viewed in the online issue, which is available at wiley onlinelibrary.com.]

actual copolymer matrix. Figure 8 shows that the current is almost constant after half hour reduction for both latex films by coating 16 and 12 mL solution on cathode, respectively. This indicated stable migration resistance of Cu^{2+} ions through SCF. Referred to the porous structure of SCF, the resistance should be mainly from solid architecture in SCF. However, the sum of solid architecture thickness over the total cross-section of SCF is much less than the total size of pores. Their length ratio should be 1 of 20, referred to the same figure. When Cu^{2+} ions migrate in SCF, the two transportation mechanisms were suggested according to previous publications[21–23]: ion penetration among macromolecular chains or segment transportation via the rotation of macromolecular segments of the ternary copolymer. Both the mechanisms are dependent on the free volume in matrix. Undoubtedly, compared to solid SCFs, in our previous studies,[24,25] this porous matrix has two advantages: (1) it decreases the net penetration distance in SCF and (2) the lower glass transition temperature of the ternary copolymer provides the easy segment rotation of the ternary copolymer. Thus, this porous morphological structure and low-T_g character of the copolymer provide the beneficial conditions for Cu^{2+} ion transportation and reduction.

With the sample in Figure 7, the element content was measured by EDS (Fig. 9) under a SEM described in Experimental section. Table I shows that the copper content is 16.36% (mol) or 49.5% (wt). XRD data (Fig. 10) confirmed the copper(0) characteristic crystal peaks at $2\theta = 36.6$, 43.4, 50.7, and 74.4. These results indicated the presence of copper (0) and its high contents in CPGCF.

Figure 11 shows that the position of Cu2p3 shifts from 935.0 eV in Cu_2SO_4 to 934.1 eV in CPGCF, and

TABLE I
The Element Content Evaluation by EDS[a]

	Percentage of elements (%)		
	C	O	Cu
By weight	42.07	7.05	49.53
By mole	73.49	9.24	16.36

[a] The total content of elements is not full percentage due to other minor components; the same sample with Figure 2.

the signal becomes much weaker in CPGCF. The position shift can be attributed to distinct interactions, depending on electron structures in Cu^{2+} and $Cu(0)$ involved. The reduced copper exists as copper nanoparticles and situates at more stable status, and thus $Cu(0)$ in CPGCF shows lower energy level. The weak and broad peak of $Cu(0)$ around 934.1 eV also shows the weaker interaction between $Cu(0)$ and hydroxyl groups in PVA.

Dependence of micromorphological structure of CPGCF on electrochemical conditions

Based on the previous investigations,[1] the morphological structure in cross-section of CPGCF depends largely on SCF structure and electrochemical conditions, including coating thickness, predrying time, and electrochemical reduction voltage. However, the porous structure in SCF will be the important factor to cause the difference from our previous publications.[10,11,24,25]

Figure 8 shows the influence of SCF thickness, in which a smaller current through electrochemical cycle was caused by thicker SCF (the bottom curve, which coated with 16 mL solution). This means the larger migration resistance of Cu^{2+} ions in SCF. Figure 12 shows the effect of predrying time on the
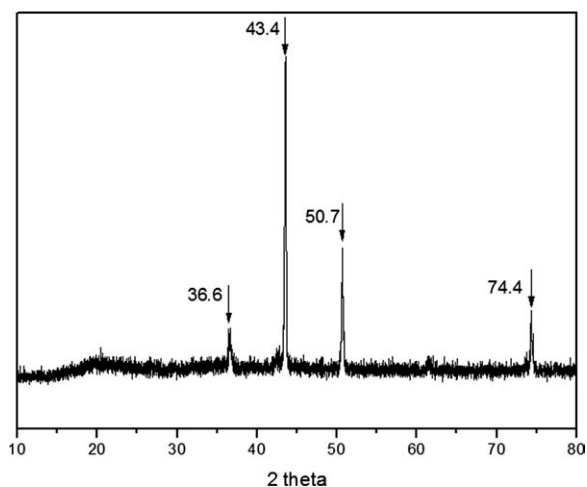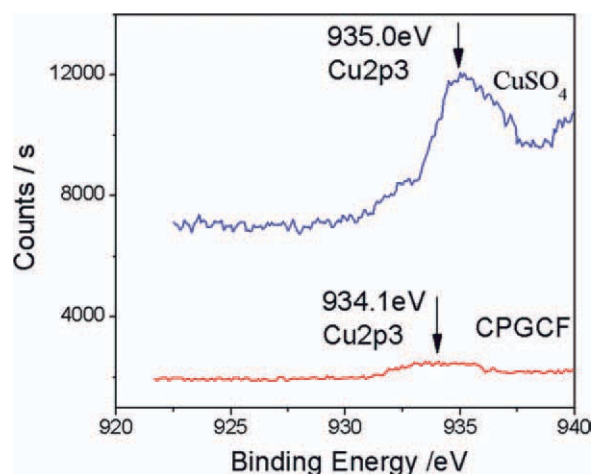

Figure 11 X-ray photoelectron spectroscopy (XPS) result of CPGCF. Sample was synthesized at the same conditions as in Figure 11 X-ray photoelectron spectroscopy (XPS) result of CPGCF. Sample was synthesized at the same conditions as in Figure 6. [Color figure can be viewed in the online issue, which is available at wileyonlinelibrary.com.]

current. The lower current was caused by longer predrying time; for example, the bottom curve presents the current of 40 h predried SCF. This trend is coincident with our previous reports.[10,11] In this work, the porous structure in SCF makes small resistance for Cu^{2+} ions to migrate as mentioned earlier, but predrying process may cause the pores close, because low T_g of the ternary copolymer. It is the main difference that predrying of SCF gives a higher resistance for Cu^{2+} ions to migrate. On the other hand, the dc voltage has obvious influence on current (Fig. 13). The larger dc voltage applied provides a larger current. As the reduction of Cu^{2+} into Cu^0 needs the minimal electropotential (0.337 V), according to basic electrolysis principle, we choose

Figure 10 Wide-angle X-ray diffraction (XRD) result of CPGCF. Sample was synthesized at the same conditions as in Figure 6.
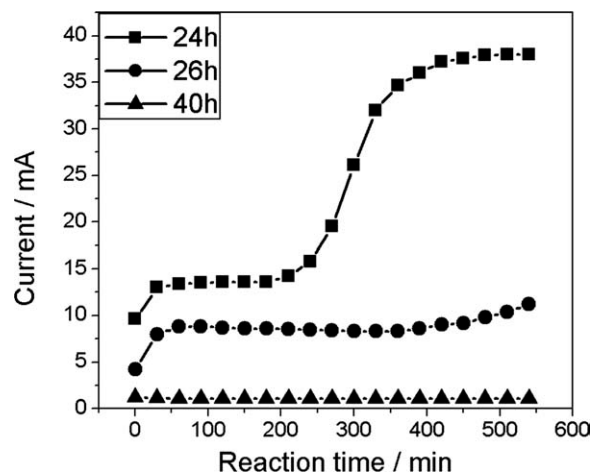

Figure 12 The effect of drying time on the current. Synthesized conditions: latex volume 14 mL; the voltage of direct electric power 0.55 V; concentration of $CuSO_4$, 150 g/L; ratio of $CuSO_4$ to HSO_4 in the electrolyte, 3 : 1.
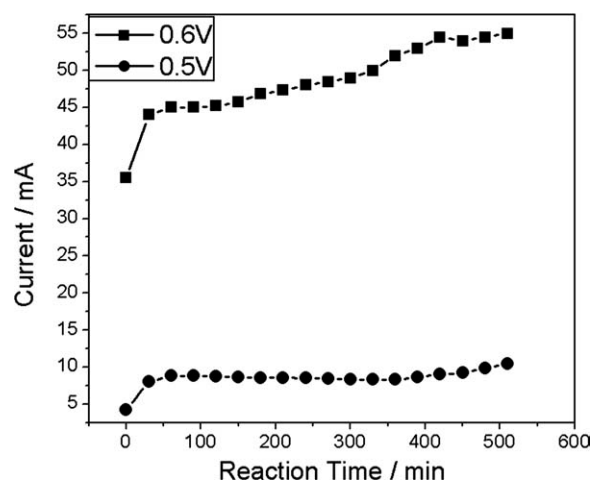
Figure 13 Change of current versus reaction time with different voltages. Synthesized conditions: predrying time of the coagulated nanolatex film, 28 h; latex volume 14 mL; concentration of $CuSO_4$, 150 g/L; ratio of $CuSO_4$ to H_2SO_4 in the electrolyte, 3 : 1; the electrochemical reduction time, 9 h.

dc voltage in the range of 0.45–0.60 V. This choice bases on the special mechanisms of ion motion stated earlier. Our experiments indicated that if the voltage exceeded 0.65 V, a great deal of hydrogen was generated that impair SCF.

CONCLUSION

CPGCF can be obtained through electrochemical strategy via reducing a SCF. Ternary copolymer consisting of styrene, butyl acrylate, and acrylic acid structural units is the matrix polymer in this SCF. Thanks to the well-emulsified nanoparticles in this copolymer latex, the coating film as SCF on cathode has rich porous structure. This porous structure improves the Cu^{2+} transportation and reduction in SCF; thus, it benefits to form a gradient distribution of reduced copper along the cross-section of SCF. After dried, the SCF becomes CPGCF. The dense copper layer embedded in the most cathode side in the ternary copolymer matrix has excellent metal property, and the flexibility of polymer is kept for the gradient composite film. Importantly, compared to our previous publications on the similar gradient

composite researches, this porous structure formed by the latex nanoparticles of the ternary copolymer is special factor to improve the copper gradient distribution in this new CPGCF.

References

1. Tang, J.; Chen, Q.; Liu, H.; Wang, Y. J Appl Polym Sci 2004, 92, 373.
2. Voevodin, A. A.; Zabinski, J. S. Diam Relat Mater 1998, 7, 463.
3. Voevodin, A. A.; Walck, S. D.; Zabinski, J. S. Wear 1997, 203, 516.
4. Papathanasiou, T. D.; Soininen, R.; Caridis, K. A. J Metal 1995, 24, 159.
5. Wu, P.; Zhou, C. Z.; Tang, X. N. Surf Coat Tech 2003, 166, 84.
6. Liu, T.; Wang, Q.; Gao, A.; Zhang, C.; Wang, C. J.; He, J. C. Scr Mater 2007, 57, 992.
7. Wang, Q.; Liu, T.; Gao, A.; Zhang, C.; Wang, C. J.; He, J. C. Scr Mater 2007, 56, 1087.
8. Chand, N.; Dwivedi, U. K.; Sharma, M. K. Wear 2007, 262, 184.
9. Chung, R. J.; Chin, T. S.; Chen, L. C.; Hsieh, M. F. Biomol Eng 2007, 24, 434.
10. Tang, J.; Hu, K.; Fu, S.; Qi, H.; Cui, W.; Jia, Z.; Li, K.; Pang. H. J Appl Polym Sci 1998, 69, 1159.
11. Tang, J.; Chu, X.; Gao, X.; Zhao, W. J Appl Polym Sci 1996, 61, 1773.
12. Tent, A. V.; Nijenhuis, K. te. J Colloid Interf Sci 2000, 232, 350.
13. Stewarda, P. A.; Hearna, J.; Wilkinsonb, M. C. Adv Colloid Interf Sci 2000, 86, 195
14. Niu, B.-J.; Urban, M. W. J Appl Polym Sci 1998, 70, 1321.
15. Woods, H. M.; Silva, M. M. C. G.; Nouvel, C.; Shakesheff, K. M.; Howdle, S. M. J Mater Chem 2004, 14, 1663.
16. Jiang, P.; Hwang, K. S.; Mittleman, D. M.; Bertone, J. F. J Am Chem Soc 1999, 121, 11630.
17. Sun, H.-B.; Xu, Y.; Ye, J.-Y.; Matsuo, S.; Misawa, H.; Song, J.; Du, G.; Liu, S. Jpn J Appl Phys 2000, 39, L591.
18. Sun, H.-B.; Song, J.; Xu, Y.; Matsuo, S.; Misawa, H.; Du, G.; Liu, S. J Opt Soc Am B: Opt Phys 2000, 17, 476.
19. Velev, O. D.; Jede, T. A.; Lobo, R. F. Chem Mater 1998, 10, 3597.
20. Pekcan, O. J Colloid Interf Sci 2002, 251, 409.
21. Doblhofer, K.; Vorotyntsev, M. In Electroactive Polymer Electrochemistry, Part 1: Fundamentals; Lyons, M. E. G., Ed.; Plenum: New York, 1994; Chapter 3, p 375–442.
22. Tang, J.Synthesis, Structure, and Properties of Metal-in-Polymer Matrix Gradient Composite Film, Dissertation for Doctoral Degree at Shanghai Jiao Tong University, 2000.
23. Li, G. C.; Zhang, P.; Zhang, H. P.; Yang, L. C.; Wu, Y. P. Electrochem Comm 2008, 10, 1883.
24. Tang, J.; Che, Y.; Liu, H.; Wang, Y. J Appl Polym Sci, 2005, 95, 539.
25. Tang, J.; Wang, D.; Wang, Y.; Liu, H.; Wang, X. J Appl Polym Sci 2006, 100, 2796.